

A Bi-Dimensional Identification Model of Seismic Vulnerability and Intelligent Sensing Capability: A Case of Seoul

Juncheng Zeng^{1,*}, Jiyeong Kang¹, Dowan Kim¹ and Hwanyong Kim^{2,*}

¹ Department of Smart City Engineering, Hanyang University ERICA, Ansan, Republic of Korea

² School of Architecture and Architectural Engineering, Hanyang University ERICA, Ansan, Republic of Korea

INFORMATION

Keywords:

Seismic vulnerability
intelligent sensing capability
urban disaster governance
smart city
Seoul

DOI: 10.23967/j.rimni.2026.10.74464

Revista Internacional
Métodos numéricos
para cálculo y diseño en ingeniería

RIMNI



UNIVERSITAT POLITÈCNICA
DE CATALUNYA
BARCELONATECH

In cooperation with
CIMNE³

A Bi-Dimensional Identification Model of Seismic Vulnerability and Intelligent Sensing Capability: A Case of Seoul

Juncheng Zeng^{1,*}, Jiyeong Kang¹, Dowan Kim¹ and Hwanyong Kim^{2,*}

¹Department of Smart City Engineering, Hanyang University ERICA, Ansan, Republic of Korea

²School of Architecture and Architectural Engineering, Hanyang University ERICA, Ansan, Republic of Korea

ABSTRACT

Seismic disasters pose increasingly complex risks to large metropolitan areas. Identifying spatial disparities between seismic vulnerability and governance capacity has become a critical issue for enhancing urban resilience. This study proposes a bi-dimensional identification model integrating seismic vulnerability and intelligent sensing capability, using the 25 districts of Seoul as a case. A comprehensive three-level indicator system of seismic vulnerability was developed. Simultaneously, the spatial density of S-DoT sensors, representing the city's intelligent sensing infrastructure, was adopted as a proxy for district-level sensing capability. Methodologically, spatial data processing was conducted using ArcGIS Pro, while Z-score standardization and K-means clustering were performed in Python. To ensure the scientific rigor of the numerical model, a multi-scenario sensitivity analysis was conducted to evaluate the impact of multicollinearity among indicators. The clustering stability was further validated through the Adjusted Rand Index (ARI) and centroid shift metrics, and cross-checked with hierarchical clustering, confirming consistent typological structures. The results identified three types: (1) high vulnerability–low sensing, (2) moderate to low vulnerability–high sensing, and (3) moderate to low vulnerability–low sensing. These types exhibited distinct spatial clustering patterns and imply differentiated governance priorities and responses. The primary contribution of this research lies in introducing a spatially coupled model that integrates intelligent sensing into seismic vulnerability assessment. This approach moves beyond traditional static, one-dimensional frameworks, offering improved visual interpretability and decision support. The findings offer insights for resilience-oriented governance in Seoul and other high-density cities.

OPEN ACCESS

Received: 11/10/2025

Accepted: 20/01/2026

DOI

10.23967/j.rimni.2026.10.74464

Keywords:

Seismic vulnerability
intelligent sensing capability
urban disaster governance
smart city
Seoul

Abbreviations

SV	Seismic Vulnerability
IoT	Internet of Things
ISC	Intelligent Sensing Capability
S-DoT	Smart Seoul Urban Data Sensor

WCSS Within-Cluster Sum of Squares
ARI Adjusted Rand Index

1 Introduction

With the continued global expansion of urbanization, natural hazards such as earthquakes are posing increasingly severe challenges to cities [1,2]. Urban seismic governance is no longer limited to traditional engineering based protection but is evolving toward a more spatially differentiated approach focusing on vulnerability identification and targeted management [3]. In recent years, substantial theoretical and empirical advances have been made in modeling urban seismic vulnerability (SV) and assessing spatial risks [4–6]. However, how to achieve precise allocation of governance resources in densely built and structurally complex urban environments remains an urgent issue to be addressed.

SV serves as a key indicator for assessing potential losses in urban systems during an earthquake. It encompasses a wide range of dimensions, including building structures, population distribution, infrastructure robustness, and socioeconomic conditions [7]. For instance, Lestuzzi et al. [8], Sandoli et al. [9], and Xofi et al. [10] emphasized the role of building typologies; Zhang et al. [11] investigated the impact of urban demographic structures; Cardoni et al. [12] focused on the vulnerability of telecommunication infrastructure; El-Maissi et al. [13] addressed the role of road networks; Baquedano Juliá et al. [14] studied the fire hazard component; Poudel et al. [15] examined medical resource availability; and Karashima et al. [16] explored intercity support capacity. These studies have proposed various indicator systems and composite scoring methodologies that offer technical approaches for identifying high risk areas. Nevertheless, most existing research tends to adopt static portrayals of spatial vulnerability, particularly building based vulnerability, and rarely incorporates the city's intrinsic capacity to perceive and recognize seismic risk. Recent studies have advanced seismic vulnerability research by extending its analytical scope from individual structures to large scale urban and infrastructural systems. For example, Li et al. [17] developed an intelligent prediction framework for reinforced concrete bridge networks using multiple machine learning algorithms; Zhang et al. [18] employed the extremely random tree algorithm to construct a spatial magnetic susceptibility model and proposed an intelligent seismic risk assessment framework; and Li et al. [19] proposed a probabilistic fragility model for building clusters under mainshock–aftershock sequences. These works have greatly enriched the methodological foundation for data driven and intelligent seismic risk assessment. Building upon these advances, the present study extends the discussion toward the spatial governance dimension by integrating seismic vulnerability with intelligent sensing capability in an urban scale framework.

In addition, recent advances in seismic risk and vulnerability research have increasingly adopted data-driven and probabilistic modeling frameworks to capture the complex interactions between seismic hazards, exposure, and resilience. In the domain of seismic risk, Rudman et al. [20] employed stochastic ground-motion simulations and Monte Carlo methods to evaluate probabilistic seismic hazard and risk, emphasizing the role of data-driven uncertainty quantification in modern seismic modeling. Karimzadeh et al. [21] developed an ANN-based ground motion model for Turkey using region-specific stochastic earthquake simulations, effectively capturing spatial and tectonic heterogeneity in ground motion prediction. In addition, Habib et al. [22] proposed a blockchain-integrated seismic risk mitigation framework for smart cities, demonstrating how decentralized real-time data management can enhance transparency, reliability, and response efficiency in disaster governance. Regarding seismic vulnerability, Li [23] developed a multidimensional probabilistic vulnerability

model for typical urban building portfolios by coupling macroseismic and instrumental intensity measures, providing refined correlation parameters for empirical damage states based on field data. Firmansyah et al. [24] introduced a CNN-based framework that classifies building typologies from ground-level imagery, achieving over 84% accuracy and enabling rapid city-scale vulnerability mapping in earthquake-prone regions. Similarly, Ferranti et al. [25] applied neural networks and random forests hybrid machine learning algorithms to infer a posteriori vulnerability scores from observed damage data, demonstrating the transferability of machine learning-based vulnerability assessment across different urban contexts. Collectively, these studies mark a methodological convergence toward intelligent, probabilistic, and cross-scale modeling of seismic risk and vulnerability. By integrating machine learning, probabilistic simulation, and digital technologies, recent research has moved beyond static empirical models, laying a solid foundation for this study's integration of intelligent sensing and spatial vulnerability assessment within a unified urban resilience framework.

Under the advancement of smart city concepts, urban sensing systems have increasingly emerged as critical infrastructure for supporting risk identification [26,27]. Intelligent sensing technologies, centered on the Internet of Things (IoT) and sensor networks, are widely deployed in domains such as environmental monitoring and traffic safety, and have gradually been applied to seismic micro vibration detection and structural health monitoring in disaster related contexts [28,29]. Recent studies have further advanced this trend by integrating intelligent sensing and deep learning models into seismic vulnerability assessment, such as the application of hybrid sensing frameworks for risk mapping, employment of integrated artificial intelligence controllers to enhance real-time responsiveness and deep learning based seismic damage prediction models [30–32]. While the functionality of these sensing devices is continuously improving, their spatial deployment often remains uneven. The degree of spatial coupling between sensing infrastructure and SV may amplify or mitigate imbalances in governance capacity [33]. Therefore, integrating SV with intelligent sensing capability (ISC) into a spatially explicit identification framework is becoming a crucial agenda in smart city research.

Some existing studies have assessed ISC from the perspectives of sensor density and coverage [34]; others have focused on mapping spatial SV [35,36]. However, there is a relative paucity of research that integrates these two dimensions into a “bi-dimensional governance capacity model” and identifies differentiated governance types through spatial clustering analysis. This gap is particularly evident in high density cities such as Seoul. The city simultaneously faces challenges from aging building stock and latent seismic risks [37], while also accelerating its development of urban sensing platforms [38], offering a fertile ground for empirical analysis.

To address this, the present study proposes a bi-dimensional identification model based on “SV–ISC” (hereafter referred to as the “Vulnerability–Intelligent” framework). By constructing a district level SV index and a sensing density indicator, the study uses the 25 autonomous districts of Seoul as the basic units of analysis. Methodologically, the spatial distribution of both indicators is visualized using heatmaps, followed by Z-score standardization and K-means clustering to identify governance typologies. Furthermore, considering the potential for multicollinearity within high-dimensional indicator systems, this study incorporates a rigorous stability diagnostic framework. By employing the Adjusted Rand Index (ARI) and centroid shift analysis across multiple perturbation scenarios, the numerical robustness of the clustering results is quantitatively validated. Finally, tailored governance strategies are proposed based on cluster characteristics, supporting precision oriented seismic governance within the context of smart cities.

2 Study Area and Data

2.1 Overview of Seoul

Seoul, the capital of South Korea, is the most populous, economically developed, and extensively built city on the Korean Peninsula. As the political, economic, and cultural center of the country, Seoul plays a pivotal role in national development. Located in the northwestern part of South Korea and bisected by the Han River, Seoul is administratively divided into 25 autonomous districts, as shown in Fig. 1c. These districts differ significantly in terms of urban functions, population density, and building structures.

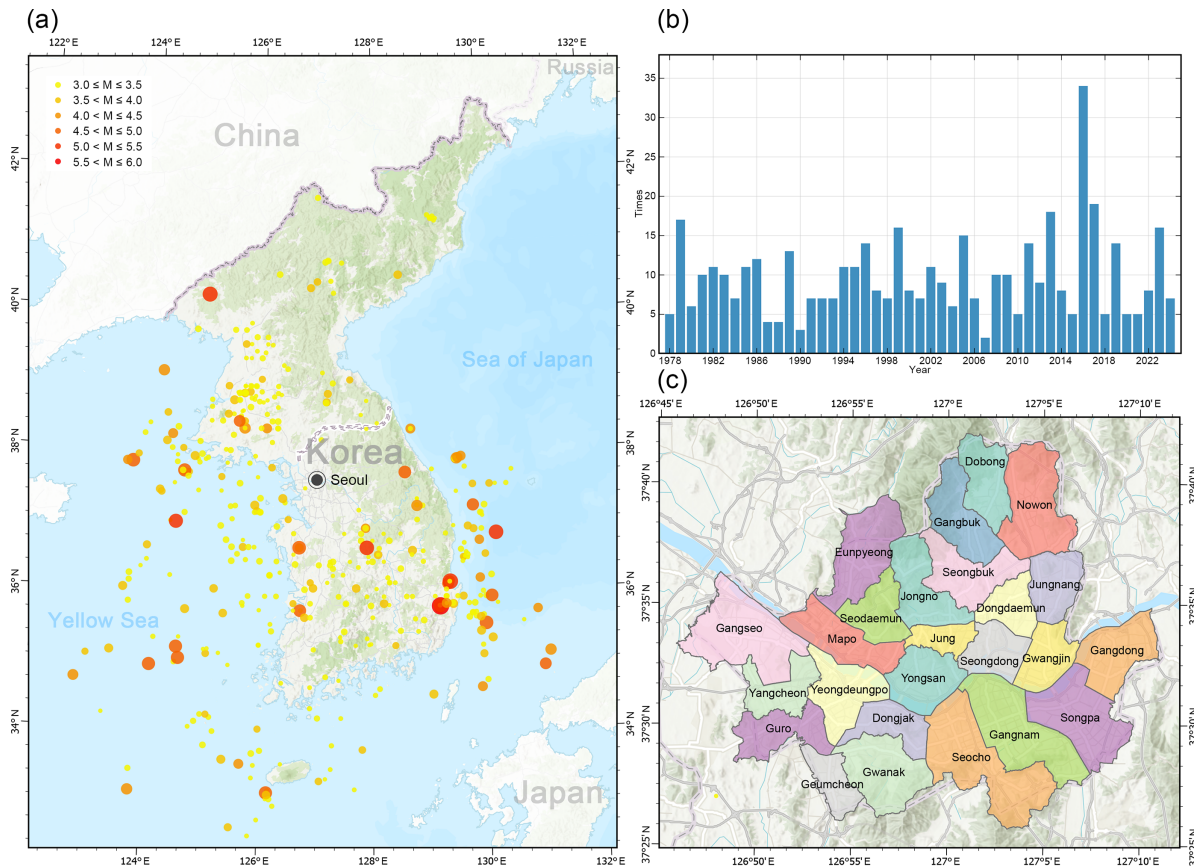


Figure 1: (a) Locations of earthquakes of magnitude 3.0 or Higher in Korea Since 1978 (Source: Korea meteorological administration); (b) annual records of earthquakes of magnitude 3.0 or higher in Korea since 1978 (Source: Korea meteorological administration); (c) administrative districts of seoul

Although Seoul lies within the relatively stable interior of the Eurasian tectonic plate and is generally considered a region of low seismic activity, it is not entirely free from tectonic influences. The presence of Quaternary faults, including the Chugaryeong fault zone [39], in and around the Seoul area indicates a certain level of underlying seismic risk. In recent years, seismic activity across the Korean Peninsula has increased, with multiple moderate magnitude earthquakes recorded since 2011. Notably, the 2016 Gyeongju Earthquake ($M = 5.8$) [40] and the 2017 Pohang Earthquake ($M = 5.4$) [41] raised public and governmental awareness of earthquake hazards [42]. These events suggest that, despite Seoul's relatively low earthquake frequency, the potential risk cannot be ignored (Fig. 1a,b).

Seoul is widely recognized as a global frontrunner in smart city development. As early as the early 2000s, the city launched its “U-city” project [43], followed by the “Smart Seoul 2015” initiative and the “Global Digital Seoul 2020” strategy [44,45]. In 2021, the city unveiled the “Seoul Vision 2030,” outlining its future oriented development agenda [46]. These policies have collectively facilitated the city’s transformation toward intelligent governance, progressing through three key stages: early stage digitalization of administrative services, mid-stage expansion of online public services, and recent upgrades in urban infrastructure driven by the IoT and big data. This evolution reflects a shift toward a more sustainable and resilience oriented governance system [47].

As a critical component of smart city construction, Seoul has recently undertaken large scale deployments of urban sensing infrastructure. A wide array of IoT sensors has been installed across bridges, roads, railways, buildings, and parks [48]. These sensors cover diverse domains such as weather and environmental conditions, air quality, noise and lighting, surface conditions, pedestrian density, vibrations, and structural stress. This multi-dimensional sensing network enables real-time monitoring of natural environments, infrastructure health, and urban activity. It provides crucial data support for environmental surveillance, risk early warning, infrastructure maintenance, and emergency response, forming the backbone of Seoul’s intelligent governance system (Fig. 2a,b).

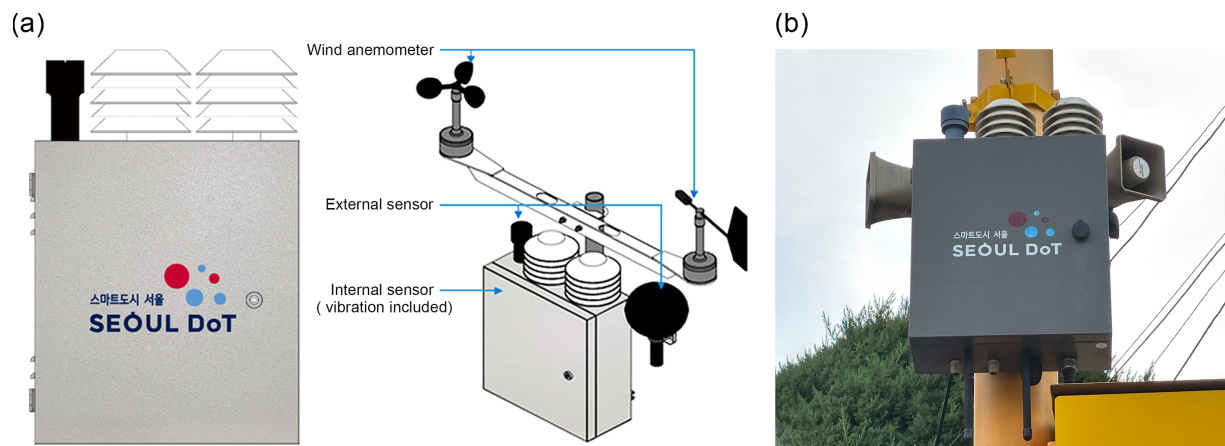


Figure 2: (a) S-DoT sensor deployment (Source: Seoul metropolitan government); (b) S-DoT sensor actual image (Source: Photograph taken by the authors)

2.2 Data

To assess SV, this study develops a comprehensive evaluation index system tailored to the urban context of Seoul, as detailed in the Section 3. The index incorporates diverse dimensions—such as building conditions, fire protection, medical capacity, population distribution, evacuation infrastructure, lifelines, economic strength, and socio-environmental factors—aiming to reflect both the exposure level and coping capacity of urban systems in the face of seismic hazards. The original datasets were sourced primarily from official government platforms in South Korea, ensuring authority, reliability, and comparability across administrative units. Specific variables and their data sources are provided in Table 1. After data cleaning and normalization, and guided by the weighting framework described later, an SV score was calculated for each of Seoul’s 25 autonomous districts, forming the foundation for spatial analysis and typology identification.

Table 1: SV data affiliations and sources

Affiliation	Source
Ministry of land, infrastructure and transport	V-world digital twin lands Building data private opening system National geographic information institute
Ministry of the interior and safety	Local administration integrated information system Public data portal National disaster and safety portal
Ministry of health and welfare	Health insurance review and assessment service National health insurance service statistical information
National fire agency	Korea fire safety big data platform
Statistics Korea	Korean statistical information service

For ISC, this study uses the “Smart Seoul Urban Data Sensor (S-DoT) Deployment Information” dataset, made publicly available via the Seoul Open Data Plaza. The S-DoT system comprises 1159 IoT-based sensors deployed throughout Seoul, monitoring a wide range of environmental conditions. These sensors include modules capable of capturing three-axis vibration data, indicating their ability to detect minor ground or structural movements. While they are not certified seismic instruments, they serve practical roles in recognizing structural disturbances and anomalous urban dynamics. In this study, ISC does not narrowly refer to pre-earthquake defense or early warning systems; rather, it emphasizes a district’s capacity for timely recognition, feedback, and response under seismic stress. The spatial density of S-DoT sensors is thus considered a valid proxy indicator for ISC, interpreted as part of the ancillary infrastructure that supports seismic risk recognition and governance responsiveness.

For administrative boundaries, the unit of analysis is Seoul’s 25 autonomous districts. Shapefile data for these districts were retrieved from the Korea National Geographic Information Institute. District level area measurements were computed using ArcGIS Pro, providing the geospatial foundation for constructing the dual-indicator “SV–ISC” analytical model.

3 Method

3.1 Construction of the Seismic Vulnerability Index

3.1.1 Development of the Seismic Vulnerability Indicator System

To systematically assess the SV of each autonomous district in Seoul, this study establishes a multi-level indicator system specifically tailored for high density urban environments. Numerous studies have shown that SV should be evaluated from multiple dimensions, as single variable assessments cannot adequately reflect the potential risks faced by urban systems [49–51].

Taking into account Seoul’s urban characteristics—such as early stage development, a large stock of aging buildings, a high prevalence of single family homes, complex urban morphology, and high population density, this study developed an indicator framework grounded in existing research

and refined through consultations with three experts in disaster vulnerability assessment and urban planning in Korea.

The final framework comprises 8 primary indicators, 16 secondary indicators, and 77 tertiary indicators, covering a wide range of dimensions including building vulnerability, fire hazard risk, evacuation vulnerability, liquefaction risk, lifeline risk, urban rescue difficulty, inter-urban support difficulty, and urban recovery difficulty. A detailed description is provided in [Table 2](#).

Table 2: SV indicator framework

Risk type	Component	Detailed indicators
Buildings vulnerability	Reinforced concrete	Building structure, roof type, seismic design, building importance, number of stories, building age, building ground condition
	Steel frame	Building structure, roof type, seismic design, building importance, number of stories, building age, building ground condition
	Timber structure	Building structure, roof type, seismic design, building importance, number of stories, building age, building ground condition
	Masonry structure	Building structure, roof type, seismic design, building importance, number of stories, building age, building ground condition
Fire hazard risk	Fire propagation	Wooden residential buildings, building coverage ratio, road width, wind speed, hazardous materials facilities, fire truck accessibility
	Fire containment	Fire-resistant structure, firefighting capacity, fire hydrants, road width, urban parks, fire response speed
Evacuation vulnerability	Urban context	Road width, seismic-resistant roads, daytime evacuation population, nighttime evacuation population, vulnerable population, emergency response capacity
	Evacuation facilities	Outdoor evacuation shelters, temporary housing facilities
Liquefaction risk	Hazardous ground	Liquefaction-prone area
Lifeline risk	Infrastructure facilities	Water supply facilities, wireless stations, substations, gas supply infrastructure

(Continued)

Table 2 (continued)

Risk type	Component	Detailed indicators
Urban rescue difficulty	Direct impact factors	Road width, seismic road infrastructure, population density, number of rescue personnel, medical staff, number of hospital beds
	Indirect impact factors	Outdoor evacuation sites, temporary housing facilities
Inter-urban support difficulty	Local support capacity Geographical accessibility	Number of public officials, firefighting capacity, number of medical personnel, number of hospital beds Euclidean distance, land transportation access, maritime transportation access, air transportation access
Urban recovery difficulty	Economic indicators	Fiscal self-reliance ratio, gross regional domestic product, number of tax filers, total tax revenue
	Socioenvironmental indicators	Home ownership rate, number of aged houses, number of single elderly households, number of wooden houses

As shown in [Table 2](#), the indicator framework comprehensively integrates multiple physical and systemic factors that influence seismic vulnerability in urban environments. The differentiation of building materials, lifeline systems, and emergency response dimensions is consistent with global research findings on seismic fragility. Studies have demonstrated that structural materials exhibit distinct seismic performance characteristics [52]. Reinforced concrete and steel structures, for example, possess higher ductility yet are prone to cumulative cyclic degradation, while masonry structures fail in a brittle manner under strong ground motion [53]. Timber buildings, though flexible and lightweight, remain particularly vulnerable to post-earthquake fire and compound hazards [54]. Moreover, post-seismic fire risk and its propagation are significantly affected by building density, construction type, and local spatial morphology [55].

Beyond building materials, lifeline systems, including bridges, gas pipelines, and water and power supply networks, are among the most critical components determining urban functionality during seismic events. Their damage and cascading failures can dramatically increase regional vulnerability [56–58]. Likewise, rescue and recovery processes are governed by accessibility, response capacity, and inter urban support networks, which directly shape post disaster resilience [59–61]. Finally, socioeconomic vulnerability complements physical exposure, as disparities in population density, income, and housing age have been shown to influence both immediate impacts and long term recovery potential [62].

These global findings collectively validate the multi-dimensional design of the proposed SV indicator framework, confirming its theoretical soundness and empirical applicability for assessing seismic vulnerability in high density metropolitan contexts such as Seoul.

3.1.2 Calculation of the Seismic Vulnerability Index

SV is inherently multidimensional and complex, influenced by various physical, social, and infrastructural factors. It is well recognized that seismic intensity measures, such as peak ground acceleration, spectral acceleration, and ground motion duration are core indicators in developing quantitative models of earthquake vulnerability and risk [63]. However, as this study focuses on intra urban spatial heterogeneity within a single metropolitan area, variations in local seismic intensity are assumed to be relatively uniform across districts. Many previous urban scale studies have similarly omitted seismic intensity variables when analyzing intra city vulnerability, arguing that the spatial variation of ground motion within a single city is negligible compared to the influence of built environment and social factors [64,65]. Therefore, instead of modeling seismic intensity explicitly, the analysis controls for it implicitly by concentrating on exposure, structural, and socioeconomic dimensions of vulnerability. This approach is consistent with urban scale seismic risk assessments where regional differences in ground motion are minimal. To ensure the constructed index is both operational and adaptable to high density metropolitan contexts, a weighted composite scoring method is employed, adopting a uniform weighting scheme at different indicator levels.

Specifically, at the primary indicator level, equal weights are assigned to all seven dimensions, reflecting the assumption that each represents an equally critical risk aspect in seismic contexts. This approach enhances the balance of the evaluation, preventing biases caused by variations in the number or richness of indicators within certain dimensions [66]. At the tertiary indicator level, the weight allocated to each primary indicator is evenly distributed across its corresponding tertiary indicators. This ensures that each observed variable has equal influence within its dimension, simplifying the evaluation process and enhancing reproducibility and applicability in other urban settings [67]. The secondary indicators, serving only as structural intermediaries for classification, are not directly involved in numerical calculation. Given that each primary indicator typically contains only 1–2 secondary indicators, assigning weights at this level would add unnecessary complexity without significant analytical value. Therefore, the weighting process deliberately omits the secondary level. To ensure comparability prior to aggregation, all tertiary indicators are normalized. To mitigate the potential bias introduced by the disparate number of tertiary indicators across different dimensions, we adopt a hierarchical compensatory aggregation logic. Let $\hat{x}_{i,j,k}$ denote the raw value of the k th tertiary indicator under the j th primary dimension for district i th. The aggregation process is formulated as a nested linear combination, ensuring that each primary dimension contributes a fixed proportion $\frac{1}{m}$ to the final SV Index, regardless of its internal cardinality. The seismic vulnerability index SV_i for district i is computed using the following weighted aggregation formula:

$$SV_i = \sum_{j=1}^m w_j \left(\frac{1}{n_j} \sum_{k=1}^{n_j} \hat{x}_{i,j,k} \right) \quad (1)$$

where:

SV_i : SV Index of district i ;

m : Total number of first level indicator dimensions;

w_j : Weight of the j th primary dimension, where $w_j = \frac{1}{m}$ for all j , satisfying $\sum w_j = 1$;

n_j : Number of third level indicators under the j th first level dimension;

$\hat{x}_{i,j,k}$: Normalized value of the j th third level indicator under the k th dimension for district i .

This formulation ensures numerical stability by localizing the variance within each dimension before global integration. By treating each primary dimension as an orthogonal vector in a 7-dimensional risk space, the model effectively reduces the impact of multicollinearity among tertiary indicators within the same component, as their internal correlations are averaged out during the dimension-level mean calculation.

3.2 Construction of the Intelligent Sensing Capability Index

The ISC Index is designed to reflect the spatial coverage and equilibrium of sensing infrastructure in urban space. In this study, the index is derived from the spatial distribution of sensors provided by the S-DoT system. The density of sensor deployment is used as a proxy for ISC, based on the assumption that higher sensor density equates to stronger environmental awareness and real-time situational monitoring—key traits of urban resilience and intelligent governance systems.

The implementation process is as follows: First, the geographic coordinates of all sensors across Seoul are extracted from the S-DoT dataset to form a point feature layer. Using Spatial Join in ArcGIS Pro, the sensor points are spatially overlaid with the polygon layer of Seoul's 25 autonomous districts. The number of sensors within each district is then computed. Next, by combining this count with the land area of each district, the sensor deployment density ISC_i (units/km²) is calculated as follows:

$$ISC_i = \frac{N_i}{A_i} \quad (2)$$

where:

ISC_i : ISC index of district i ;

N_i : Total number of S-DoT sensors deployed within district i ;

A_i : Land area of district i (in square kilometers).

This density value serves as the ISC Index for each district, forming the second axis of the subsequent dual-dimensional classification model.

3.3 Clustering Analysis Method

To identify the governance typologies of Seoul's autonomous districts under the bi-dimensional framework of SV and ISC, this study adopts the K-means clustering algorithm to classify governance priority types in a data driven manner. Given the differences in units and value ranges between the two indicators, standardization is necessary to ensure the accuracy of distance based clustering.

This study employs Z-score standardization for both SV and ISC indicators. From a numerical computation perspective, the necessity of Z-score standardization arises from the sensitivity of distance-based algorithms to the magnitude of input variables. Since SV is a composite index and ISC represents a physical density (units/km²), their raw scales are non-commensurable. Without standardization, the objective function of the clustering algorithm would be dominated by the variable with the larger absolute variance, leading to a biased partition of the feature space. The Z-score method transforms each variable into a standard normal distribution with a mean of 0 and a standard deviation of 1 ($\mu = 0, \sigma = 1$), thereby mapping the observations into a dimensionless isotropic Euclidean space where the distance metric is equally sensitive to both dimensions. The standardization is calculated using the formula:

$$Z_i = \frac{X_i - \mu}{\sigma} \quad (3)$$

where:

Z_i : Standardized value of the i th observation;

X_i : Original value of the i th observation;

μ : Mean of the variable;

σ : Standard deviation of the variable.

The resulting two-dimensional standardized vectors are then used as inputs for the clustering analysis.

The input variables consist of the standardized Z-score values of SV and ISC for each of Seoul's 25 autonomous districts, forming a two-dimensional attribute matrix $X = [Z_{SV}, Z_{ISC}]$. The output is the categorical cluster label C_i assigned to each district, representing distinct governance typologies characterized by combinations of vulnerability and sensing capability. Conceptually, these clusters correspond to different urban governance configurations.

K-means is a classical unsupervised learning algorithm based on Euclidean distance. In the context of this study, the dataset is represented as a set of $N = 25$ observations $\{z_1, z_2, \dots, z_N\}$, where each z_i is a two-dimensional real vector $[z_{SV}, z_{ISC}]^T$ representing the standardized coordinates. The algorithm seeks to find a partition $S = \{S_1, S_2, \dots, S_K\}$ that minimizes the Within-Cluster Sum of Squares (WCSS), which is equivalent to minimizing the trace of the within-cluster scatter matrix. This property aligns well with the objective of identifying functionally distinct yet internally coherent governance regions, thereby supporting the typological recognition of seismic resilience patterns within Seoul's urban system. The objective function can be expressed as:

$$J = \sum_{k=1}^K \sum_{z_i \in S_k} \|z_i - \mu_k\|^2 \quad (4)$$

where:

J : The objective function value, representing the WCSS;

S_k : The k th cluster;

μ_k : The centroid (mean vector) of the k th cluster;

z_i : A standardized attribute vector assigned to cluster S_k ;

$\|\cdot\|$: Euclidean norm (distance).

The optimization is achieved through an iterative Lloyd's algorithm, consisting of an assignment step (Voronoi partition) and an update step (centroid re-calculation). This numerical approach ensures that the resulting typologies are not mere heuristic groupings but represent local minima of the total variance in the bi-dimensional risk-sensing space. To validate the numerical stability of the clusters, we use the Elbow Method to identify the inflection point of the $J(K)$ function, where the marginal gain in variance reduction diminishes significantly. The algorithm updates cluster centroids μ_k iteratively until the assignment stabilizes or the objective function converges.

In this study, the analysis is conducted on 25 autonomous districts of Seoul, with each sample represented by a pair of standardized values (Z_{SV}, Z_{ISC}) in the two-dimensional indicator space. To determine the optimal number of clusters K , the Elbow Method is employed. This involves calculating SSE for a range of K values and plotting the results to identify the "elbow point", the value of K at which the decrease in SSE begins to level off. This point indicates the most appropriate number of clusters for interpretation and policy analysis.

3.4 Robustness and Sensitivity Analysis Method

To quantitatively evaluate the robustness of the bi-dimensional model and address the potential impact of multicollinearity among the 77 tertiary indicators, a sensitivity analysis framework is introduced. We define the stability of the clustering results through three mathematical dimensions:

First, the Cluster Stability Index is measured by the Centroid Shift ($\Delta\mu$), which quantifies the geometric displacement of cluster centroids in the standardized feature space after removing redundant indicators:

$$\Delta\mu_k = \sqrt{\sum_{p \in \{SV, ISC\}} (\mu_{k,p} - \mu'_{k,p})^2} \quad (5)$$

where:

$\Delta\mu_k$: The centroid shift of the k th cluster in the standardized bi-dimensional space;

$p \in \{SV, ISC\}$: The dimensions of the feature space;

$\mu_{k,p}$: The original centroid coordinate of cluster K on dimension p calculated using the full indicator set;

$\mu'_{k,p}$: The new centroid coordinate of cluster K on dimension p after removing highly correlated indicators.

Second, to identify the redundant variables for the stress test, the linear dependency between any two indicators is quantified using the Pearson correlation coefficient (r):

$$r_{xy} = \frac{\sum_{i=1}^n (x_i - \bar{x})(y_i - \bar{y})}{\sqrt{\sum_{i=1}^n (x_i - \bar{x})^2 \sum_{i=1}^n (y_i - \bar{y})^2}} \quad (6)$$

where:

r_{xy} : The Pearson correlation coefficient between indicator x and indicator y ;

n : The total number of administrative districts;

x_i, y_i : The standardized values of the i th district for indicators x and y ;

\bar{x}, \bar{y} : The mean values of the respective indicators across all districts.

Finally, the classification consistency before and after the perturbation is evaluated using the Adjusted Rand Index (ARI), which measures the similarity between two clustering partitions while accounting for chance grouping:

$$ARI = \frac{\sum_{ij} \binom{n_{ij}}{2} - \left[\sum_i \binom{a_i}{2} \sum_j \binom{b_j}{2} \right] / \binom{n}{2}}{\frac{1}{2} \left[\sum_i \binom{a_i}{2} + \sum_j \binom{b_j}{2} \right] - \left[\sum_i \binom{a_i}{2} \sum_j \binom{b_j}{2} \right] / \binom{n}{2}} \quad (7)$$

where:

ARI : The index value ranging from -1 to 1 (where 1 indicates perfect agreement);

n_{ij} : The number of districts that are assigned to the same cluster in both the original and the perturbed models;

a_i, b_j : The sums of the rows and columns in the contingency table of the two clustering results;

$\binom{n}{2}$: The binomial coefficient representing the total number of possible district pairs.

These metrics provide a comprehensive numerical diagnostic for the model’s sensitivity to multi-collinearity. Conceptually, a small $\Delta\mu_k$ relative to the inter-cluster distance, combined with a high *ARI* value, indicates superior numerical stability. This proves that the multi-level equal-weight aggregation effectively mitigates the impact of redundant variables, ensuring that the resulting urban governance typologies are driven by the underlying spatial structure of risk and sensing infrastructure rather than the overrepresentation of specific correlated indicators. The technology roadmap is shown in Fig. 3.

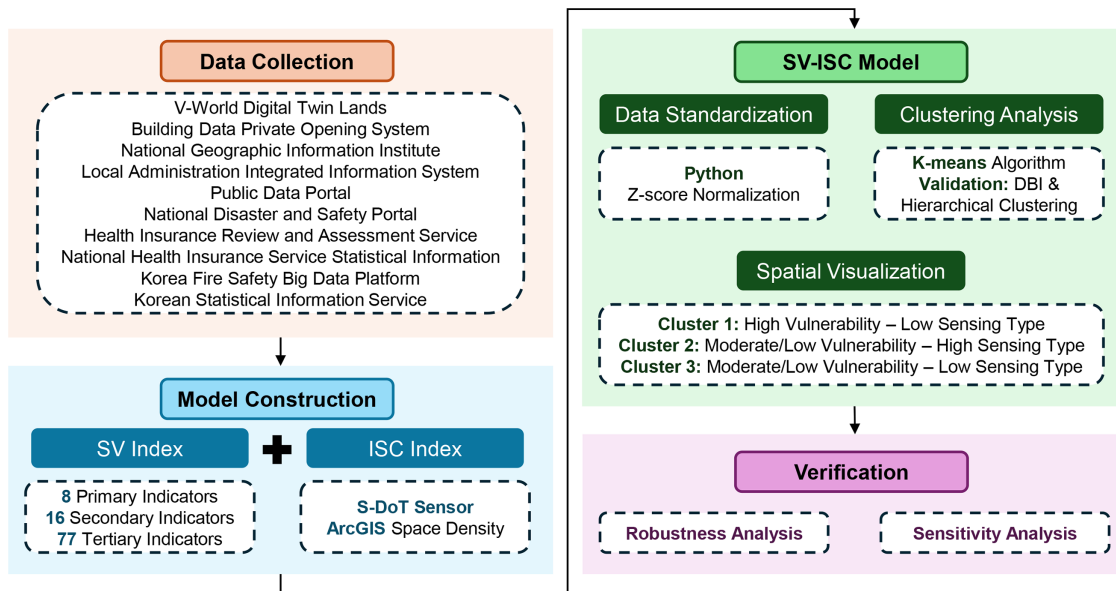


Figure 3: Technology roadmap

4 Results

4.1 Seismic Vulnerability

By calculating the SV score for each autonomous district in Seoul, the results reveal a certain degree of spatial autocorrelation. The districts of Gangnam-gu and the adjacent Seocho-gu exhibit the highest SV values, indicating heightened SV. Conversely, Yeongdeungpo-gu and its neighboring Guro-gu show the lowest SV values. Overall, the eastern part of Seoul tends to have higher SV, while the western areas demonstrate relatively lower SV levels (see Fig. 4).

4.2 Intelligent Sensing Capability

The ISC score for each district was computed based on sensor density. Yangcheon-gu recorded the highest ISC value (4.828 units/km²), whereas Seocho-gu showed the lowest (0.896 units/km²). Notably, historic northern districts along the Han River, including Jung-gu, Seongdong-gu, Mapo-gu, Jongno-gu, and Dongdaemun-gu, exhibited higher ISC values. In contrast, business intensive southern districts such as Seocho-gu, Gangnam-gu, and Songpa-gu demonstrated lower levels of ISC (see Fig. 5).

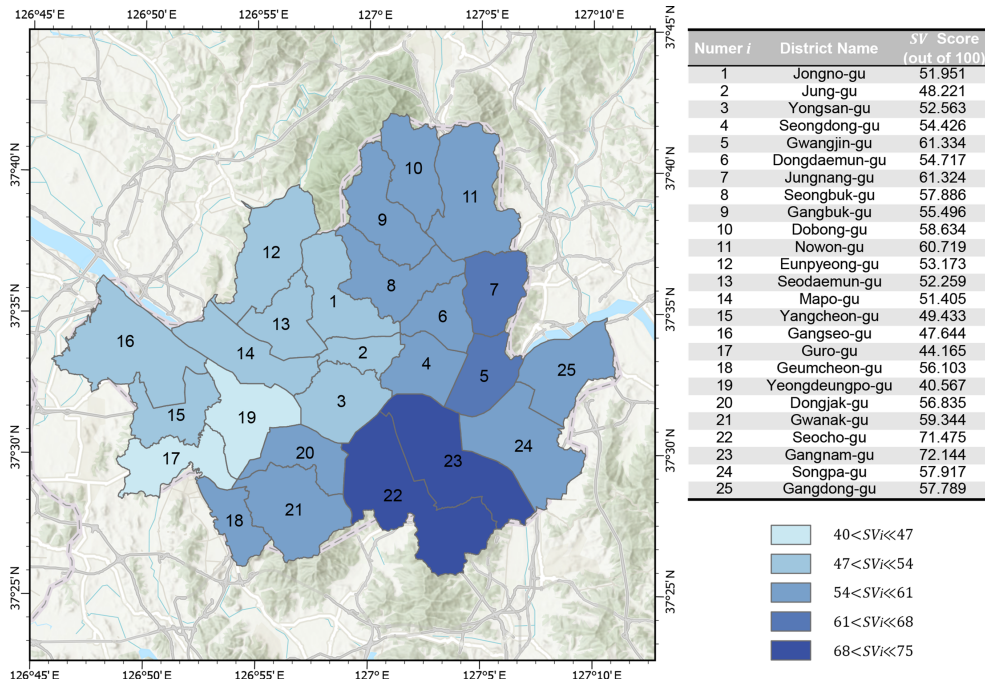


Figure 4: SV score by district in Seoul

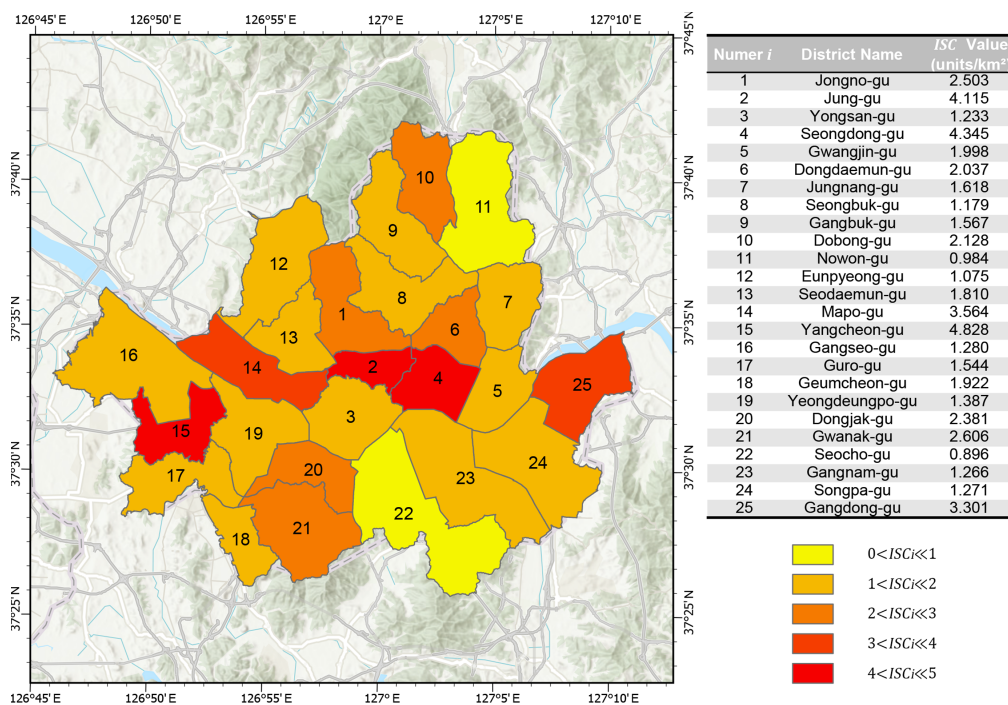


Figure 5: ISC value by district in Seoul

4.3 Clustering and Typology

4.3.1 Z-Score Standardization

To categorize Seoul's 25 districts based on their performance in the dual-dimensional framework of SV and ISC, we applied K-means clustering. Since K-means is a distance based unsupervised algorithm, it is sensitive to scale differences across variables. Therefore, prior to clustering, both SV and ISC indicators were standardized using Z-score normalization, which transforms the data into a standard distribution with a mean of 0 and a standard deviation of 1.

It is worth noting that although the SV index was initially calculated based on normalized (Min-Max) tertiary indicators, the final index still differs in scale from ISC values. Thus, applying Z-score normalization remains necessary to ensure comparability across variables. The standardized results for both SV and ISC are presented in [Table 3](#).

Table 3: Z-score normalization results of SV and ISC across Seoul districts

Numer i	District name	Z_{sv}	Z_{isc}
1	Jongno-gu	-0.506	0.359
2	Jung-gu	-1.038	1.843
3	Yongsan-gu	-0.419	-0.811
4	Seongdong-gu	-0.153	2.055
5	Gwangjin-gu	0.832	-0.106
6	Dongdaemun-gu	-0.112	-0.07
7	Jungnang-gu	0.83	-0.456
8	Seongbuk-gu	0.34	-0.86
9	Gangbuk-gu	-0.001	-0.503
10	Dobong-gu	0.447	0.013
11	Nowon-gu	0.744	-1.04
12	Eunpyeong-gu	-0.332	-0.956
13	Seodaemun-gu	-0.462	-0.279
14	Mapo-gu	-0.584	1.336
15	Yangcheon-gu	-0.865	2.499
16	Gangseo-gu	-1.12	-0.767
17	Guro-gu	-1.616	-0.524
18	Geumcheon-gu	0.086	-0.176
19	Yeongdeungpo-gu	-2.129	-0.669
20	Dongjak-gu	0.19	0.246
21	Gwanak-gu	0.548	0.453
22	Seocho-gu	2.278	-1.121
23	Gangnam-gu	2.373	-0.78
24	Songpa-gu	0.345	-0.776
25	Gangdong-gu	0.326	1.093

4.3.2 Determining the Optimal Number of Clusters

Before performing clustering, the Elbow Method was used to identify the optimal number of clusters (K). By plotting the within cluster sum of squares (SSE) for different values of K , we observed that the SSE significantly decreased from $K = 1$ to $K = 3$, after which the marginal improvement diminished. The curve notably flattened beyond $K = 3$, indicating a clear “elbow” at this point (see Fig. 6). Thus, $K = 3$ was selected as the optimal balance between information retention and model simplicity.

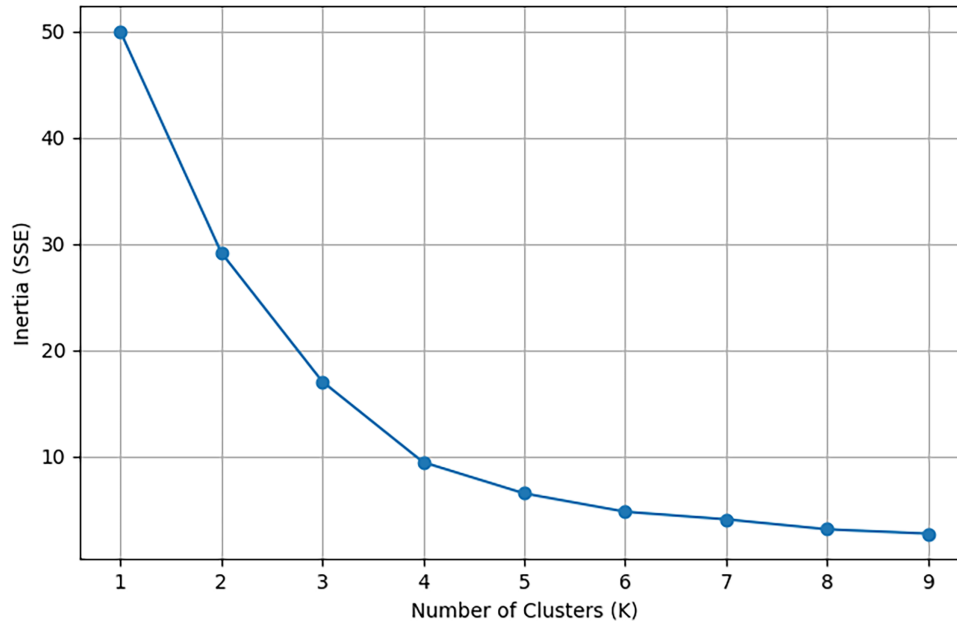


Figure 6: Elbow method for optimal K

4.3.3 K-Means Clustering

Based on the Z-score standardized values of SV and ISC, K-means clustering with $K = 3$ was conducted using Python. To mitigate the impact of random initialization, n_init was set to 10, meaning the algorithm was run 10 times with different centroid seeds, and the solution with the lowest total error (SSE) was retained, ensuring robustness and reliability of the results.

The clustering performance was first evaluated using the Davies–Bouldin Index (DBI), which yielded a value of 0.850. As a lower DBI value indicates better inter cluster separation and intra cluster cohesion, and values below 1.0 are generally considered indicative of acceptable clustering performance [68], this result confirms the stability and reliability of the K-means classification.

To further confirm the robustness of the classification, a comparative test was performed using the hierarchical clustering (Ward linkage) algorithm. As shown in Table 4, the classification patterns produced by both methods were largely consistent, most of the districts assigned to identical or functionally equivalent clusters. Minor differences were observed only in cluster labeling, not in the underlying spatial or functional grouping. This high degree of consistency demonstrates that the typological segmentation derived from the bi-dimensional framework is stable and not sensitive to the choice of clustering algorithm. K-means was ultimately selected as the primary analytical method,

as it is widely adopted in urban typology and governance classification studies for its computational efficiency, interpretability, and suitability for continuous quantitative indicators [69,70].

Table 4: Comparison of clustering results from K-means and hierarchical clustering

Numer i	District name	K-means cluster	Hierarchical cluster
1	Jongno-gu	3	3
2	Jung-gu	2	2
3	Yongsan-gu	3	3
4	Seongdong-gu	2	2
5	Gwangjin-gu	1	3
6	Dongdaemun-gu	3	3
7	Jungnang-gu	1	3
8	Seongbuk-gu	1	3
9	Gangbuk-gu	3	3
10	Dobong-gu	1	3
11	Nowon-gu	1	3
12	Eunpyeong-gu	3	3
13	Seodaemun-gu	3	3
14	Mapo-gu	2	2
15	Yangcheon-gu	2	2
16	Gangseo-gu	3	3
17	Guro-gu	3	3
18	Geumcheon-gu	1	3
19	Yeongdeungpo-gu	3	3
20	Dongjak-gu	1	3
21	Gwanak-gu	1	3
22	Seocho-gu	1	1
23	Gangnam-gu	1	1
24	Songpa-gu	1	3
25	Gangdong-gu	2	2

As shown in Fig. 7, data points in the two-dimensional space of SV and ISC exhibit clear convergence around their respective cluster centers. A spatial visualization of clustering outcomes (see Fig. 8) reveals noticeable spatial clustering patterns: Cluster 1 is primarily located in the eastern and southern parts of Seoul. Cluster 2 is mostly distributed along the Han River, forming a belt-like structure. Cluster 3 is mainly concentrated in the western and northwestern regions.

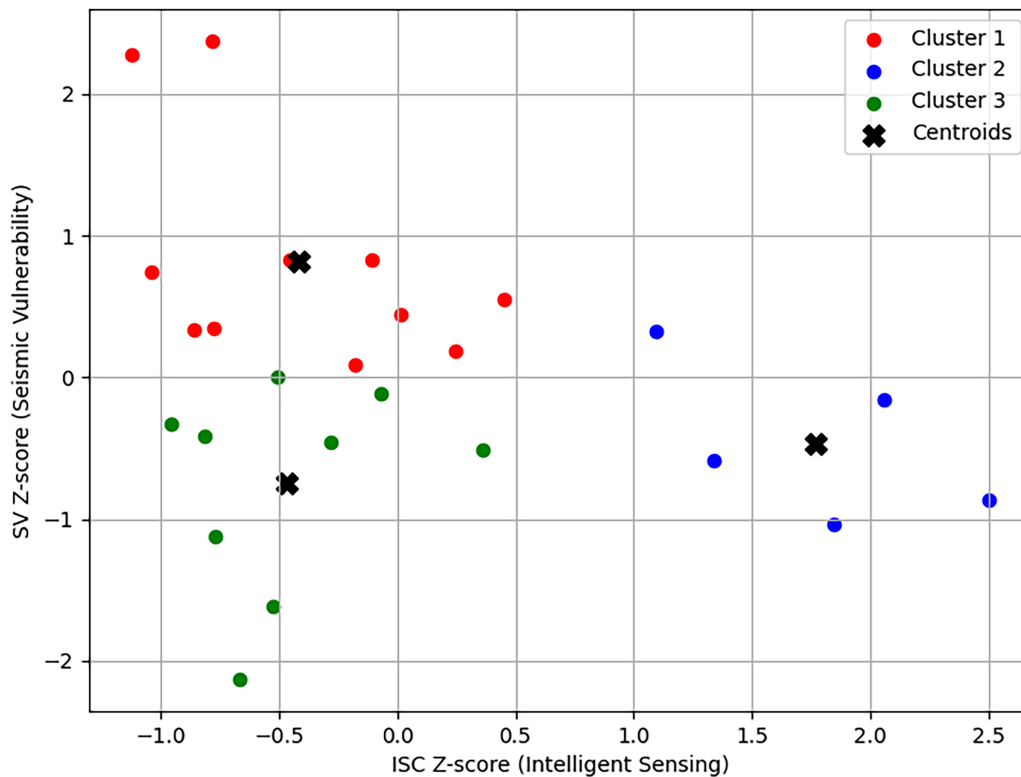


Figure 7: K-means clustering (k = 3)

Based on the centroid positions and standardized indicator values, the three clusters can be interpreted as follows:

1. Cluster 1 (High Vulnerability—Low Sensing Type): Districts in this cluster show high SV but low levels of ISC. These are priority areas for seismic governance interventions. Typical cases include Seocho-gu and Gangnam-gu, where it is recommended to prioritize the deployment of sensing infrastructure and retrofitting of vulnerable structures.
2. Cluster 2 (Moderate/Low Vulnerability—High Sensing Type): These districts feature strong ISC coverage and relatively low SV. Representative areas such as Seongdong-gu and Yangcheon-gu serve as ideal pilot zones for resilient urban governance under smart city frameworks.
3. Cluster 3 (Moderate/Low Vulnerability—Low Sensing Type): These areas have average SV but insufficient sensing infrastructure. Examples include Eunpyeong-gu and Gangseo-gu. Gradual investments in sensing technologies and multi-source data integration are recommended to strengthen their emergency preparedness and digital governance capabilities.

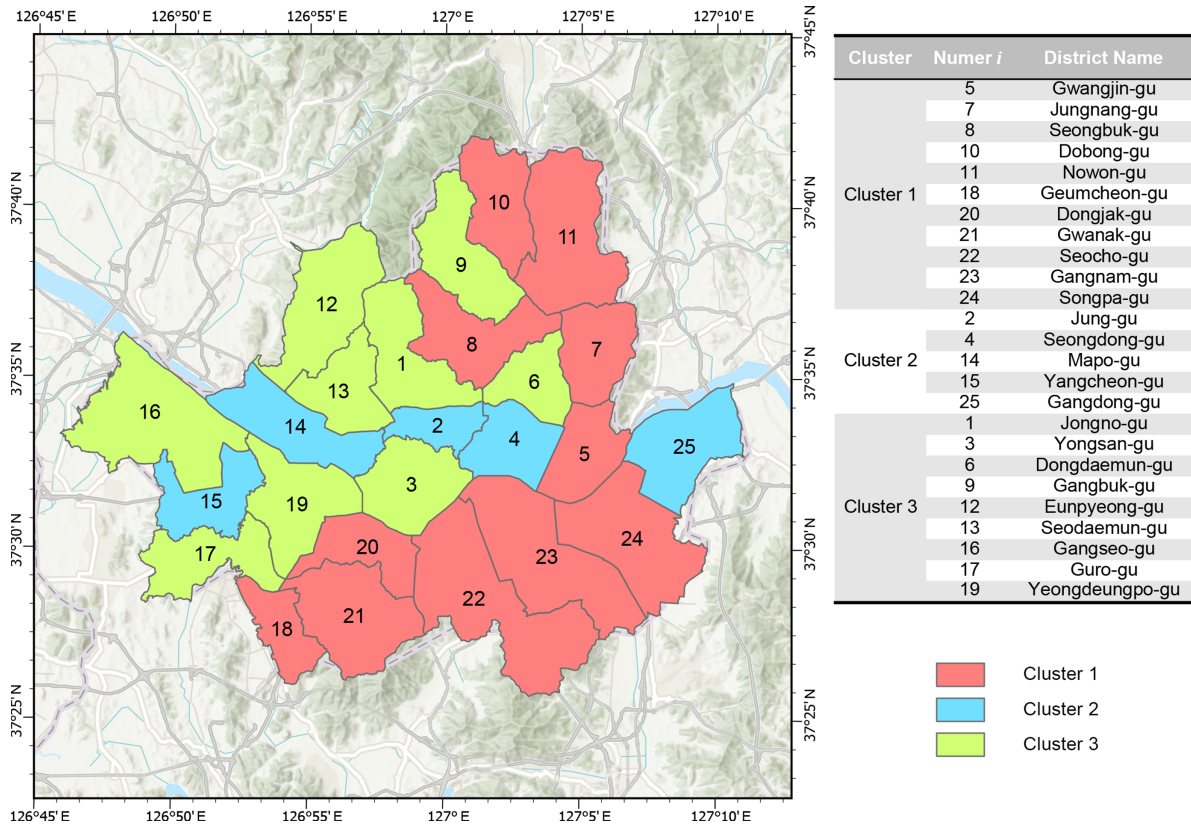


Figure 8: SV–ISC cluster types across districts in Seoul

4.4 Robustness and Sensitivity Analysis

To address the concern regarding multicollinearity, we first identified indicators with high linear dependencies. Table 5 lists the top five indicator pairs with the highest Pearson correlation coefficients (r) found in the dataset.

Table 5: Top five highly correlated indicator pairs

Rank	Indicator pair	Pearson r
1	Wooden residential buildings & fire-resistant structure	0.9931
2	Emergency response capacity & number of tax filers	0.9495
3	Masonry structure & liquefaction-prone area	0.9173
4	Fiscal self-reliance ratio & gross regional domestic product	0.8782
5	Wireless stations & substations	0.8728

Subsequently, a gradient-based sensitivity test was conducted to evaluate if these redundancies affect the final classification. We simulated three scenarios (Cases A, B, and C) by shielding these indicators and re-running the clustering optimization. The results are summarized in Table 6.

Table 6: Numerical stability and sensitivity analysis results

Scenario	Indicators removed	Max centroid shift ($\Delta\mu_{\max}$)	Adjusted rand index (<i>ARI</i>)
Baseline	Full indicator set	0	1
Case A	Top 1 pairs	0.0165	1
Case B	Top 3 pairs	0.0382	1
Case C	Top 5 pairs	0.0574	0.96

The diagnostic results identified five representative high-correlation pairs across different dimensions, with the highest correlation observed between indicator Wooden Residential Buildings and Fire-resistant Structure ($r = 0.9931$). To rigorously test the model’s robustness, we simulated three scenarios by gradually removing these redundant variables. As summarized in Table 6, the maximum centroid shift ($\Delta\mu_{\max}$) reached 0.0574 in the most extreme case (Case C), which remains significantly lower than the inter-cluster distances. The *ARI* remained as high as 0.96, confirming that the classification of Seoul’s 25 districts is not contingent on specific redundant indicators but reflects the stable, underlying urban characteristics. These findings effectively address the concerns regarding multicollinearity and confirm the reliability of the equal-weight aggregation approach.

5 Discussion

This study constructed a bi-dimensional index system integrating SV and ISC, and applied K-means clustering to classify 25 autonomous districts in Seoul into governance relevant spatial types. The results show that the three clusters exhibit significant structural differences in both risk levels and sensing capabilities, reflecting strong spatial orientation and practical applicability for urban governance. Based on this, the following discussion focuses on governance prioritization, sensing capability development, and sensing resource allocation strategies, aiming to offer practical insights for resilient smart city governance. Furthermore, to enhance the robustness and generalization of the proposed framework, the discussion extends to model scalability, algorithmic performance validation, and global implementation perspectives.

5.1 Governance Logic and Policy Implications behind Cluster Types

Based on the clustering analysis, three combined types of “SV–ISC” configurations were clearly identified across Seoul. In “High Vulnerability—Low Sensing” districts, the urgency for seismic risk governance is the greatest, making them top priority zones for resilience enhancement. In contrast, “Moderate/Low Vulnerability—High Sensing” areas exhibit robust foundations for disaster governance, rendering them ideal testbeds for pilot innovations in intelligent seismic governance. Districts of the “Moderate/Low Vulnerability—Low Sensing” type may not pose immediate threats but still require attention to address structural deficiencies and prevent future accumulated risks.

Thus, the significance of clustering lies not only in classification, but also in guiding differentiated policy investment pathways. This helps avoid the pitfalls of “equal resource distribution” and instead supports a shift toward a more targeted “identification–prioritization–response” governance loop.

From a planning perspective, the typological results provide a decision support foundation for developing localized resilience strategies that align with Seoul’s broader urban safety and smart infrastructure plans. This direction is highly consistent with Seoul Smart City’s ongoing initiatives,

such as the S-DoT network and the “Smart City & Digitization Master Plan (2021–2025),” which emphasize integrated urban sensing, data-driven safety management, and adaptive risk governance [71]. Internationally, similar frameworks are being implemented in New York Smart City projects, where IoT-based environmental monitoring and urban analytics are utilized to strengthen emergency response and predictive resilience planning [72]. Likewise, Singapore’s Smart Nation initiative demonstrates the integration of AI-driven urban analytics, pervasive sensing, and real-time data platforms to enhance public service delivery and urban resilience [73].

Similar approaches could be applied in other cities with comparable governance structures, such as Tokyo and Taipei, where high density metropolitan areas located along the Pacific Ring of Fire, characterized by elevated seismic risk and a relatively advanced level of technological capacity.

5.2 Governance Pathways for High Vulnerability—Low Sensing Areas

For districts classified as High Vulnerability—Low Sensing, their dual disadvantages considerably amplify the systemic risks posed by seismic events. These areas should be prioritized in resilience building strategies.

First, basic sensing infrastructure must be urgently deployed. Sensor resources should be directed toward neighborhoods with dense aging buildings, high population concentration, and poor emergency accessibility to fill the gaps in sensing coverage. Second, a multi-source sensing system should be integrated—encompassing structural health monitoring, ambient seismic detection, and underground pressure monitoring via diverse IoT nodes—to enable early anomaly detection. Third, a data-closed-loop mechanism linking sensing systems with emergency response platforms should be established, ensuring that risk perception can trigger timely governance actions.

Governance efforts in these districts should not rely solely on physical infrastructure; instead, emphasis should be placed on embedding intelligent governance mechanisms and fostering cross sectoral collaboration. By embedding adaptive governance algorithms and predictive analytics, such as machine learning based seismic forecasting models recently applied in urban areas [74,75], future iterations of this framework can improve real time decision support and predictive resilience planning.

5.3 Spatial and Vulnerability Oriented Allocation of Sensing Resources

The deployment of intelligent sensing systems should not pursue equal distribution, but rather be guided by spatial risk mapping and urban resilience weaknesses. Based on the clustering results, the following allocation strategies are recommended:

1. **Spatial Orientation Principle:** Prioritize sensor deployment in seismic prone belts, areas near active faults, and zones with complex geological conditions.
2. **Vulnerability Orientation Principle:** Allocate more sensing resources to districts with above average SV scores, intensifying sensing coverage where vulnerability is high.
3. **Synergistic Enhancement Principle:** In areas already equipped with adequate sensing infrastructure, focus on functional expansion. For example, integrating seismic early warning systems with traffic management modules, rather than simply increasing node density.
4. **Technological Foresight Principle:** Looking forward, autonomous and adaptive sensing systems, such as 3D printed sensor modules, drone assisted deployment units, and self-organizing

IoT networks, offer new opportunities for scalable, flexible, and post event reconfigurable monitoring. These technologies enable rapid production, localized customization, and resilience-oriented recovery, enhancing the redundancy and adaptability of seismic monitoring frameworks in smart cities.

From a methodological standpoint, the clustering structure derived from the SV–ISC framework demonstrates stable and interpretable performance. Quantitatively, the high stability of the typological outputs is a direct result of the model’s ability to handle high-dimensional urban data. In the context of “numerical computational methods,” the dual-index framework successfully addressed potential multicollinearity among the 77 tertiary indicators. Our sensitivity analysis revealed that the ARI remained high even after the strategic removal of the most redundant variables. This suggests that the K-means algorithm, when combined with Z-score standardization and hierarchical equal-weight aggregation, can effectively filter out “numerical noise” and focus on the fundamental spatial disparities of the city. Such numerical robustness is crucial for smart city governance, as it ensures that policy shifts are triggered by actual changes in urban risk profiles rather than statistical artifacts or data redundancies. The model’s typological outputs remain consistent under alternative unsupervised configurations, such as hierarchical clustering, confirming its robustness and internal reliability. This consistency indicates that the proposed model is not overly sensitive to algorithmic variation and therefore possesses adequate generalization capability for broader urban applications. By ensuring that governance typologies are both functionally meaningful and methodologically stable, the framework strengthens its applicability for real world seismic governance analysis.

At a global level, the proposed SV–ISC bi-dimensional model can serve as a transferable decision-support tool for optimizing sensing resource distribution in other high density cities with available IoT infrastructure. By adjusting the weighting parameters and spatial unit definitions, the framework can be adapted to different geographies. Thus, the model facilitates a transition from quantity driven to function driven and risk aware sensing deployment strategies in smart city governance.

6 Conclusion

This study examined urban seismic governance from the perspective of coupling SV with ISC, and proposed a spatial identification model under this dual-indicator framework.

First, a multi-level SV index system was established, tailored for high-density urban environments like Seoul. The framework incorporates eight dimensions: building vulnerability, fire hazard risk, evacuation vulnerability, liquefaction risk, lifeline risk, urban rescue difficulty, inter-urban support difficulty, and urban recovery difficulty, across primary, secondary, and tertiary levels. This provides a robust quantitative tool for identifying internal urban risk heterogeneity. Second, the study introduced a novel ISC indicator derived from S-DoT sensor deployment density, reflecting the spatial capacity for environmental perception and disaster response. This led to the formation of a “SV–ISC” dual-index model for analyzing spatial disparities in governance capacity. By integrating K-means clustering, the study identified three governance types with significant spatial structure differences and proposed corresponding sensor deployment and seismic governance strategies.

Methodologically, this research integrates spatial visualization and data mining, achieving a complete loop from raw data to policy recommendation. Quantitatively, the clustering achieved a Davies–Bouldin Index of 0.850, indicating reliable internal cohesion and inter-cluster distinction. The model’s reliability was further strengthened by a rigorous sensitivity analysis targeting multicollinearity. The results yielded an ARI of 0.96 and a maximum centroid shift of 0.057 under

gradient perturbation scenarios, confirming the high numerical stability of the classification. The model's classification accuracy was further confirmed by cross-validation with hierarchical clustering. These metrics collectively demonstrate the robustness and reproducibility of the proposed learning framework. The approach balances interpretability and technical robustness, offering a scalable and replicable framework for future urban resilience assessments.

Its generalization potential lies in its adaptability to other cities where seismic risk interacts with digital sensing infrastructure, allowing policymakers to assess urban readiness under the “Vulnerability–Intelligence” paradigm. From a policy perspective, the identified cluster types offer clear guidance for targeted resource allocation: “High Vulnerability–Low Sensing” areas should be prioritized for infrastructure reinforcement, while “High Sensing–Low Vulnerability” regions can serve as demonstration zones for intelligent disaster management innovation.

Nevertheless, several limitations remain. First, the evaluation of ISC is based on the S-DoT system, which is currently only available in Seoul and not yet extended nationwide. Cross-regional comparability remains limited. Second, while S-DoT sensors include vibration detection features, they are not dedicated seismic instruments. Their function lies in supporting intelligent governance through spatial detection and rapid feedback, not traditional seismic early warning. Therefore, the ISC dimension should be interpreted as reflecting the city's capability for real-time spatial recognition and response, rather than direct pre-disaster defense. Finally, the model currently adopts static indicators; incorporating dynamic temporal data and machine learning based predictive modules could significantly enhance its forward-looking capacity and forecasting precision.

Future research could be expanded in three directions. First, refine the spatial resolution to the autonomous district level within Seoul for enhanced spatial precision and policy relevance. Second, scale the model to cover other Korean cities or the entire country to assess its generalizability and adaptability. Third, integrate data driven predictive analytics and global IoT sensor networks to develop a “Vulnerability–Resource–Capacity” 3D framework, linking physical resilience, digital readiness, and social equity under the evolving paradigm of smart and adaptive urban governance.

Acknowledgement: Not applicable.

Funding Statement: This research was funded by the Basic Research Program through the National Research Foundation of Korea (NRF), grant number RS-2023-00220751.

Author Contributions: The authors confirm contribution to the paper as follows: Conceptualization, Juncheng Zeng and Jiyeong Kang; methodology, Juncheng Zeng; software, Juncheng Zeng and Dowan Kim; validation, Juncheng Zeng and Dowan Kim; formal analysis, Juncheng Zeng and Jiyeong Kang; investigation, Dowan Kim and Hwanyong Kim; resources, Hwanyong Kim; data curation, Juncheng Zeng and Dowan Kim; writing—original draft preparation, Juncheng Zeng and Dowan Kim; writing—review and editing, Jiyeong Kang and Hwanyong Kim; visualization, Juncheng Zeng; supervision, Dowan Kim; project administration, Jiyeong Kang; funding acquisition, Hwanyong Kim. All authors reviewed and approved the final version of the manuscript.

Availability of Data and Materials: The data that support the findings of this study are available from the Corresponding Author, Juncheng Zeng, upon reasonable request.

Ethics Approval: Not applicable.

Conflicts of Interest: The authors declare no conflicts of interest.

References

1. Mori F, Gena A, Mendicelli A, Naso G, Spina D. Seismic emergency system evaluation: the role of seismic hazard and local effects. *Eng Geol.* 2020;270(1):105587. doi:10.1016/j.enggeo.2020.105587.
2. Berzhinskaya LP, Radziminovich YB, Salandayeva OI, Novopashina AV, Lukhneva OF, Ivanova NV. Comprehensive assessment of seismic hazard and vulnerability of construction objects as a prospect for further urban planning of territories. *Seism Instrum.* 2022;58(3):350–61. doi:10.3103/S0747923922030045.
3. Hoyos MC, Hernandez AF. Seismic risk assessment of multiple cities: biases in the vulnerability derivation methods for urban areas with different hazard levels. *Front Earth Sci.* 2022;10:910118. doi:10.3389/feart.2022.910118.
4. Leggieri V, Mastrodonato G, Uva G. GIS multisource data for the seismic vulnerability assessment of buildings at the urban scale. *Buildings.* 2022;12(5):523. doi:10.3390/buildings12050523.
5. Doğan A, Başeğmez M, Aydın CC. Assessment of the seismic vulnerability in an urban area with the integration of machine learning methods and GIS. *Nat Hazards.* 2025;121(8):9613–52. doi:10.1007/s11069-025-07185-4.
6. Chu J, Zhang Q, Wang A, Yu H. A hybrid intelligent model for urban seismic risk assessment from the perspective of possibility and vulnerability based on particle swarm optimization. *Sci Program.* 2021;2021:2218044. doi:10.1155/2021/2218044.
7. Duzgun HSB, Yucemen MS, Kalaycioglu HS, Celik K, Kemec S, Ertugay K, et al. An integrated earthquake vulnerability assessment framework for urban areas. *Nat Hazards.* 2011;59(2):917–47. doi:10.1007/s11069-011-9808-6.
8. Lestuzzi P, Podestà S, Luchini C, Garofano A, Kazantzidou-Firtinidou D, Bozzano C, et al. Seismic vulnerability assessment at urban scale for two typical Swiss cities using Risk-UE methodology. *Nat Hazards.* 2016;84(1):249–69. doi:10.1007/s11069-016-2420-z.
9. Sandoli A, Calderoni B, Lignola GP, Prota A. Seismic vulnerability assessment of minor Italian urban centres: development of urban fragility curves. *Bull Earthq Eng.* 2022;20(10):5017–46. doi:10.1007/s10518-022-01385-0.
10. Xofi M, Ferreira TM, Domingues JC, Santos PP, Pereira S, Oliveira SC, et al. On the seismic vulnerability assessment of urban areas using census data: the Lisbon metropolitan area as a pilot study area. *J Earthq Eng.* 2024;28(1):242–65. doi:10.1080/13632469.2023.2197078.
11. Zhang X, Tang W, Huang Y, Zhang Q, Duffield CF, Li J, et al. Understanding the causes of vulnerabilities for enhancing social-physical resilience: lessons from the Wenchuan earthquake. In: *Earthquake disasters.* London, UK: Routledge; 2021. p. 24–41. doi:10.4324/9781003173328-3.
12. Cardoni A, Borlera SL, Malandrino F, Cimellaro GP. Seismic vulnerability and resilience assessment of urban telecommunication networks. *Sustain Cities Soc.* 2022;77(4):103540. doi:10.1016/j.scs.2021.103540.
13. El-Maissi AM, Argyroudis SA, Kassem MM, Mohamed Nazri F. Integrated seismic vulnerability assessment of road network in complex built environment toward more resilient cities. *Sustain Cities Soc.* 2023;89:104363. doi:10.1016/j.scs.2022.104363.
14. Baquedano Juliá P, Ferreira TM, Rodrigues H. Post-earthquake fire risk assessment of historic urban areas: a scenario-based analysis applied to the Historic City Centre of Leiria. *Portugal Int J Disaster Risk Reduct.* 2021;60(2):102287. doi:10.1016/j.ijdr.2021.102287.
15. Poudel A, Argyroudis S, Ptilakis K. Systemic seismic risk assessment of urban healthcare system considering interdependencies to critical infrastructures. *Int J Disaster Risk Reduct.* 2024;103:104304. doi:10.1016/j.ijdr.2024.104304.
16. Karashima K, Ohgai A. A methodology of workshops to explore mutual assistance activities for earthquake disaster mitigation. *Int J Environ Res Public Health.* 2021;18(7):3814. doi:10.3390/ijerph18073814.

17. Li SQ, Han JC, Li YR, Qin PF. Intelligent prediction and evaluation models for the seismic risk and vulnerability of reinforced concrete girder bridges in large-scale zones. *Reliab Eng Syst Saf.* 2025;256:110743. doi:10.1016/j.res.2024.110743.
18. Zhang X, Huang S, Gao B, Qian H. Intelligent risk assessment of co-seismic landslide susceptibility using multi-directional seismic ground motion parameters. *Georisk Assess Manag Risk Eng Syst Geohazards.* 2025;2025:1–24. doi:10.1080/17499518.2025.2567480.
19. Li SQ, Zheng LL. Seismic fragility analysis of building clusters considering the effects of mainshock-aftershock sequences. *Struct Saf.* 2026;118:102647. doi:10.1016/j.strusafe.2025.102647.
20. Rudman A, Douglas J, Tubaldi E. The assessment of probabilistic seismic risk using ground-motion simulations via a Monte Carlo approach. *Nat Hazards.* 2024;120(7):6833–52. doi:10.1007/s11069-024-06497-1.
21. Karimzadeh S, Mohammadi A, Hussaini SMS, Caicedo D, Askan A, Lourenço PB. ANN-based ground motion model for Turkey using stochastic simulation of earthquakes. *Geophys J Int.* 2023;236(1):413–29. doi:10.1093/gji/ggad432.
22. Habib A, Alnaemi A, Habib M. Developing a framework for integrating blockchain technology into earthquake risk mitigation and disaster management strategies of smart cities. *Smart Sustain Built Environ.* 2025;14(5):1513–37. doi:10.1108/sasbe-12-2023-0376.
23. Li SQ. Seismic risk and vulnerability models considering typical urban building portfolios. *Bull Earthq Eng.* 2024;22(6):2867–902. doi:10.1007/s10518-024-01880-6.
24. Firmansyah HR, Sarli PW, Twinanda AP, Santoso D, Imran I. Building typology classification using convolutional neural networks utilizing multiple ground-level image process for city-scale rapid seismic vulnerability assessment. *Eng Appl Artif Intell.* 2024;131:107824. doi:10.1016/j.engappai.2023.107824.
25. Ferranti G, Greco A, Pluchino A, Rapisarda A, Scibilia A. Seismic vulnerability assessment at an urban scale by means of machine learning techniques. *Buildings.* 2024;14(2):309. doi:10.3390/buildings14020309.
26. Damaševičius R, Bacanin N, Misra S. From sensors to safety: internet of emergency services (IoES) for emergency response and disaster management. *J Sens Actuator Netw.* 2023;12(3):41. doi:10.3390/jsan12030041.
27. Geiss C, Jilge M, Lakes T, Taubenbock H. Estimation of seismic vulnerability levels of urban structures with multisensor remote sensing. *IEEE J Sel Top Appl Earth Obs Remote Sens.* 2016;9(5):1913–36. doi:10.1109/jstars.2015.2442584.
28. Alshaimi A, Houda M, Waqar A, Hayat S, Ahmed Waris F, Benjeddou O. Internet of Things (IoT) driven structural health monitoring for enhanced seismic resilience: a rigorous functional analysis and implementation framework. *Results Eng.* 2024;22:102340. doi:10.1016/j.rineng.2024.102340.
29. Pwavodi J, Ibrahim AU, Pwavodi PC, Al-Turjman F, Mohand-Said A. The role of artificial intelligence and IoT in prediction of earthquakes: review. *Artif Intell Geosci.* 2024;5:100075. doi:10.1016/j.aiig.2024.100075.
30. Ansari A, Zahoor F, Rao KS, Rathod GW, Mir BA. Integrating MHVSR and MSOR techniques with JFIM for seismic vulnerability assessment of sites and buildings in Jammu and Kashmir, NW Himalayas. *Phys Chem Earth Parts A/B/C.* 2025;140:104062. doi:10.1016/j.pce.2025.104062.
31. Mamat N, Abdulghafor R, Turaev S, Yakub F. Comparative review of intelligent structural safety in building seismic risk mitigation utilizing an integrated artificial intelligence controller. *Discov Appl Sci.* 2025;7(5):393. doi:10.1007/s42452-025-06914-5.
32. Ansari A, Rao KS, Jain AK, Ansari A. Deep learning model for predicting tunnel damages and track serviceability under seismic environment. *Model Earth Syst Environ.* 2023;9(1):1349–68. doi:10.1007/s40808-022-01556-7.
33. Vitor Silva AT. Designing equitable and dynamic rapid earthquake loss assessment systems. In: *Proceedings of the 14th International Conference on Applications of Statistics and Probability in Civil Engineering (ICASP14)*; 2023 Jul 9–13; Dublin, Ireland.

34. Khalifeh A, Darabkh KA, Khasawneh AM, Alqaisieh I, Salameh M, AlAbdala A, et al. Wireless sensor networks for smart cities: network design, implementation and performance evaluation. *Electronics*. 2021;10(2):218. doi:10.3390/electronics10020218.
35. Karpouza M, Chousianitis K, Bathrellos GD, Skilodimou HD, Kaviris G, Antonarakou A. Hazard zonation mapping of earthquake-induced secondary effects using spatial multi-criteria analysis. *Nat Hazards*. 2021;109(1):637–69. doi:10.1007/s11069-021-04852-0.
36. Kim B, Hong TK, Lee J, Park S, Lee J. Potential seismic hazard in Seoul, South Korea: a comprehensive analysis of geology, seismic, and geophysical field observations, historical earthquakes, and strong ground motions. *Bull Seismol Soc Am*. 2024;114(2):982–1002. doi:10.1785/0120230015.
37. Kim J, Nam S, Lee D. Current status of old housing for low-income elderly households in Seoul and green remodeling support plan: economic analysis considering the social cost of green remodeling. *Buildings*. 2022;12(1):29. doi:10.3390/buildings12010029.
38. Yoo Y. Toward sustainable governance: strategic analysis of the smart City Seoul Portal in Korea. *Sustainability*. 2021;13(11):5886. doi:10.3390/su13115886.
39. Park S, Baek I, Hong TK. Six major historical earthquakes in the Seoul metropolitan area during the Joseon dynasty (1392–1910). *Bull Seismol Soc Am*. 2020;110(6):3037–49. doi:10.1785/0120200004.
40. Son M, Cho CS, Shin JS, Rhee HM, Sheen DH. Spatiotemporal distribution of events during the first three months of the 2016 Gyeongju, Korea, earthquake sequence. *Bull Seismol Soc Am*. 2018;108(1):210–7. doi:10.1785/0120170107.
41. Grigoli F, Cesca S, Rinaldi AP, Manconi A, López-Comino JA, Clinton JF, et al. The November 2017 M_w 5.5 Pohang earthquake: a possible case of induced seismicity in South Korea. *Science*. 2018;360(6392):1003–6. doi:10.1126/science.aat2010.
42. Lee K, Ha M, Han J, Lee C. Analysis of Korean citizens' preparedness for earthquake hazards. *J Korean Earth Sci Soc*. 2022;43(1):199–209. doi:10.5467/jkess.2022.43.1.199.
43. Shin DH, Kim T editors. Enabling the smart city: the progress of u-city in Korea. In: *Proceedings of the 6th International Conference on Ubiquitous Information Management and Communication*; 2012 Feb 20–22; Kuala Lumpur Malaysia. doi:10.1145/2184751.2184872.
44. Adnan YM, Hamzah H, Dali MM, Daud MN, Alias A. Comparative overview of smart cities initiatives: Singapore and Seoul. In: *Proceedings of the International Real Estate Researchers Symposium (IRERS) 2016*; 2016 Apr 26–28; Kuala Lumpur, Malaysia.
45. Joo YM. Developmentalist smart cities? The cases of Singapore and Seoul. *Int J Urban Sci*. 2023;27(1):164–82. doi:10.1080/12265934.2021.1925143.
46. de Almeida GGF. Cities and territorial brand in the metaverse: the metaverse SEOUL case. *Sustainability*. 2023;15(13):10116. doi:10.3390/su151310116.
47. Lim Y, Edelenbos J, Gianoli A. Dynamics in the governance of smart cities: insights from South Korean smart cities. *Int J Urban Sci*. 2023;27(sup1):183–205. doi:10.1080/12265934.2022.2063158.
48. Robinson T, Ji M. Smart city Seoul: solving the urban puzzle. In: *Sustainable, smart and solidary Seoul: transforming an Asian megacity*. Cham, Switzerland: Springer International Publishing; 2022. p. 99–134. doi:10.1007/978-3-031-13595-8_5.
49. Barbat AH, Carreño ML, Pujades LG, Lantada N, Cardona OD, Marulanda MC. Seismic vulnerability and risk evaluation methods for urban areas. A review with application to a pilot area. *Struct Infrastruct Eng*. 2010;6(1–2):17–38. doi:10.1080/15732470802663763.
50. Kassem MM, Mohamed Nazri F, Noroozinejad Farsangi E. The seismic vulnerability assessment methodologies: a state-of-the-art review. *Ain Shams Eng J*. 2020;11(4):849–64. doi:10.1016/j.asej.2020.04.001.
51. Vicente R, Parodi S, Lagomarsino S, Varum H, Silva JARM. Seismic vulnerability and risk assessment: case study of the historic city centre of Coimbra. *Portugal Bull Earthq Eng*. 2011;9(4):1067–96. doi:10.1007/s10518-010-9233-3.

52. Pianese G, Chieffo N, Milani G, Partov D, Formisano A. Seismic vulnerability assessment of historical buildings in Sofia: a multi-methodological approach. *J Build Eng.* 2025;101:111834. doi:10.1016/j.jobe.2025.111834.
53. Zain M, Prasittisopin L, Mehmood T, Ngamkhanong C, Keawsawasvong S, Thongchom C. A novel framework for effective structural vulnerability assessment of tubular structures using machine learning algorithms (GA and ANN) for hybrid simulations. *Nonlinear Eng.* 2024;13(1):20220365. doi:10.1515/nleng-2022-0365.
54. Kürüm Varolgüneş F, Varolgüneş S. Post-earthquake fires (PEFs) in the built environment: a systematic and thematic review of structural risk, urban impact, and resilience strategies. *Fire.* 2025;8(6):233. doi:10.3390/fire8060233.
55. Kang T, Kang J, Lee K, Kim H, Shin J. Investigation of fire-following earthquake risk considering building and regional characteristics. *KSCE J Civ Eng.* 2026;30(2):100329. doi:10.1016/j.kscej.2025.100329.
56. Alemdar KD. Seismic risk assessment of transportation networks for the impending Istanbul earthquake with GIS-based MCDM approach. *Nat Hazards.* 2025;121(9):10085–123. doi:10.1007/s11069-025-07199-y.
57. Kwong NS, Jaiswal KS. Assessing earthquake risks to lifeline infrastructure systems in the United States. *Int J Crit Infrastruct Prot.* 2025;49(3):100758. doi:10.1016/j.ijcip.2025.100758.
58. Tehrani ZM, Tehrani GM, Dorostian A, Akashe B, Almasian M. Analyzing safety and resilience of the lifeline networks during the earthquake sequence. *Nat Hazards.* 2025;121(7):8091–109. doi:10.1007/s11069-024-07047-5.
59. Yousefi MH, Behnam B, Farahani S. An auxiliary framework to facilitate earthquake search and rescue operations in urban regions. *Nat Hazards.* 2024;120(12):11107–31. doi:10.1007/s11069-024-06619-9.
60. Liu B, Chen X, Zhou Z, Tang M, Li S. Research on disaster resilience of earthquake-stricken areas in Longmenshan fault zone based on GIS. In: *Environmental hazards and resilience.* London, UK: Routledge; 2021. p. 91–110. doi:10.4324/9781003171430-5.
61. Shen W, Li D, Yin J, Jian Y, Miao X, Yao D. Analysis of the spatiotemporal pattern of the gathering and dispersal of evacuated people in large and medium-sized cities after strong earthquakes. In: *Structural seismic and civil engineering research.* Boca Raton, FL, USA: CRC Press; 2023. p. 501–11. doi:10.1201/9781003384342-64.
62. Sousa ML, Tsionis G. National seismic risk assessment: an overview and practical guide. *Nat Hazards.* 2025;121(19):23513–46. doi:10.1007/s11069-024-07008-y.
63. Li SQ, Han JC, Li YR, Qin PF, Chen YS. Estimating the seismic vulnerability of buildings considering modified intensity measures. *Structures.* 2025;71:107989. doi:10.1016/j.istruc.2024.107989.
64. Aloisio A, De Santis Y, Irti F, Pasca DP, Scimia L, Fragiacomio M. Machine learning predictions of code-based seismic vulnerability for reinforced concrete and masonry buildings: insights from a 300-building database. *Eng Struct.* 2024;301:117295. doi:10.1016/j.engstruct.2023.117295.
65. Ma M, Zhang Y, Zhang J, Li M, Zhu J, Wang Y. Assessment of urban seismic social vulnerability based on game theory combination and TOPSIS model: a case study of Changchun City. *Sci Rep.* 2025;15(1):8189. doi:10.1038/s41598-025-92372-3.
66. DelSole T, Yang X, Tippett MK. Is unequal weighting significantly better than equal weighting for multi-model forecasting? *Quart J Royal Meteorol Soc.* 2013;139(670):176–83. doi:10.1002/qj.1961.
67. Mukhametzhanov I. Specific character of objective methods for determining weights of criteria in MCDM problems: entropy, CRITIC and SD. *Decis Mak Appl Manag Eng.* 2021;4(2):76–105. doi:10.31181/dmame210402076i.
68. Wijaya FB, Budiaji W, Wicaksono AS. Applied machine learning DBSCAN for identifying clusters of micro and small industries. *RIGGS J Artif Intell Digit Bus.* 2025;4(2):380–6. doi:10.31004/riggs.v4i2.515.
69. Han H. Adoption of K-means clustering algorithm in smart city security analysis and mythical experience analysis of urban image. *PLoS One.* 2025;20(3):e0319620. doi:10.1371/journal.pone.0319620.

70. Keller F, Nepomuceno TCC, de Carvalho VDH. A refined k-means clustering approach for optimizing urban police facility placement. *Decis Anal J.* 2025;16:100603. doi:10.1016/j.dajour.2025.100603.
71. Lee Y, Han S, Cho Y. Navigating the path to smart and sustainable cities: insights from South Korea's national strategic smart city program. *Land.* 2025;14(5):928. doi:10.3390/land14050928.
72. Zaman M, Puryear N, Abdelwahed S, Zohrabi N. A review of IoT-based smart city development and management. *Smart Cities.* 2024;7(3):1462–501. doi:10.3390/smartcities7030061.
73. Das D, Kwek B. AI and data-driven urbanism: the Singapore experience. *Digit Geogr Soc.* 2024;7:100104. doi:10.1016/j.diggeo.2024.100104.
74. Zain M, Dackermann U, Prasittisopin L. Machine learning (ML) algorithms for seismic vulnerability assessment of school buildings in high-intensity seismic zones. *Structures.* 2024;70:107639. doi:10.1016/j.istruc.2024.107639.
75. Asadollahzadeh D, Behnam B. Machine learning approaches for seismic vulnerability assessment of urban buildings: a comparative study with analytic hierarchy process. *Prog Disaster Sci.* 2025;25:100398. doi:10.1016/j.pdisas.2024.100398.